

# MAGNETORESISTIVITY IN MAGNETIC METALS

## Theoretical principles and a high accuracy method

J. B. SOUSA, J. M. MOREIRA

Centro de Física da Universidade do Porto, 4000 Porto, Portugal

(Received 31 December 1985)

**ABSTRACT**—The paper reviews basic physical mechanisms underlying magnetoresistivity in normal and magnetic metals. It describes an experimental high accuracy system implemented in our laboratory and discusses some typical results of magnetoresistivity measurements in magnetic metals; brief comments on their interpretation are also presented.

### 1 — INTRODUCTION

When a magnetic field  $\mathbf{H}$  is applied to a metal, small changes occur in the value of the electrical resistivity, originating the so called magnetoresistivity coefficient at temperature  $T$ ,

$$\Delta\rho/\rho = [\rho(T, \mathbf{H}) - \rho(T, 0)] / \rho(T, 0) \quad (1)$$

In a non-magnetic metal the change in resistivity is caused essentially by the curvature of the electron trajectories produced by the magnetic field (Lorentz force) [1-3]. The magnetoresistance then increases with the sample purity (larger electron mean free paths), as confirmed by experiment.

In a magnetic metal, besides the curvature effect (normal magnetoresistivity), two extra contributions are usually observed in  $\Delta\rho/\rho$ .

Taking a simple ferromagnetic metal with localized magnetic moments  $\mathbf{m}_i$  below the Curie point ( $T < T_c$ ), the first extra contribution arises from an *orientational* effect of  $\mathbf{H}$  in the spontaneous magnetization ( $\mathbf{M}_s$ ), as the scattering of an electron (wavevector  $\mathbf{k}$ ) with a magnetic ionic moment  $\mathbf{m}_i$  usually depends on the angle between  $\mathbf{k}$  and  $\mathbf{m}_i$  [4, 5]. Since the thermal average  $\langle \mathbf{m}_i \rangle$  has a definite direction in each magnetic domain, the

change of such directions produced by the applied field slightly modifies the intrinsic electric resistivity of each domain, therefore the sample resistivity. This effect is easy to observe in soft magnetic metals, for which  $\mathbf{M}_s$  rotates easily under the application of  $\mathbf{H}$  (low magnetic anisotropy).

Besides this orientational effect, the field  $\mathbf{H}$  also reduces the (thermal) spin fluctuations in the system. The resulting increase in the magnetic order usually produces a decrease in the electrical resistivity (fluctuation effect) (\*). This magnetoresistivity should be bigger in the vicinity of a magnetic transition point, where the spin fluctuations dominate [5, 6].

Magnetoresistance data can be usually related to fundamental aspects of the electronic and/or magnetic structure of the metal under investigation.

In normal metals, direct information can be obtained on the Fermi surface structure (open and closed electron orbits; shape and connectivity) when the measurements are performed at low temperatures and in high purity samples [2, 7, 8].

In magnetic metals, magnetoresistivity measurements enable the study of fairly diverse problems, ranging from magnetic anisotropy constants [11] and spin reorientation transitions [12], to critical phenomena and corresponding exponents near the Curie or Néel transition points [13]; when magnetic interactions compete, magnetoresistance studies may give fairly detailed information on the succession of different magnetic structures under the application of an increasing magnetic field [14, 15].

The magnetoresistivity effects are usually fairly small, both in normal and magnetic metals, corresponding to variations in the electrical resistivity of the order of  $10^{-10} - 10^{-11} \Omega \cdot \text{m}$  per  $10^6 \text{ Am}^{-1}$  applied field (corresponding to  $B \sim 1$  Tesla). The smallness of the effect puts stringent conditions on the experimental technique, and corresponding accuracy, particularly for detailed studies of the structure of  $\Delta\rho/\rho$  curves, either as a function of  $H$  or temperature.

In section 2 of this paper a brief account is presented on the basic physical mechanisms underlying the behaviour of the magnetoresistivity in normal and magnetic metals. In section 3

---

(\*) In ferromagnetic metals with large conduction electron wavelengths, the increase in magnetic order may produce an increase in  $\rho$ , due to coherence effects in the electron scattering by different magnetic moments [9, 10].

we describe in detail an experimental system implemented to measure  $\Delta\rho/\rho$  with great accuracy, with an automatic recording unit. In section 4 we present various applications of the magnetoresistivity measurements in magnetic metals, making brief comments on the physical information provided in each case.

## 2 — PHYSICAL ORIGIN OF THE MAGNETORESISTIVITY

### 2.1 — *Phenomenological equations*

#### Normal metals

In general, the electrical fields causing transport phenomena are sufficiently weak to be valid a linear approximation,

$$E_i = \rho_{ik} j_k \quad (2)$$

between the components  $E_i$  of the electrical field ( $\mathbf{E}$ ) and the components  $j_k$  of the electrical current density ( $\mathbf{j}$ ). The quantities  $\rho_{ik}$  define the generalized electrical resistivity tensor for the material under consideration. Isothermic conditions are assumed here and repetition of the  $k$ -index indicates a sum over the values (1, 2, 3). In the presence of an internal magnetic induction ( $\mathbf{B}$ ) caused by the applied magnetic field ( $\mathbf{H}$ ), the resistivity tensor obeys the Onsager relations  $\rho_{ik}(\mathbf{B}) = \rho_{ki}(-\mathbf{B})$ .

Separating  $\rho_{ik}$  into a symmetrical and an antisymmetrical part (in  $\mathbf{B}$ ), and having in mind that the effect of a magnetic field is usually fairly small, we can expand the resistivity tensor components in power of  $B_i$ , obtaining, to second order in  $\mathbf{B}$ , the result [16, 17],

$$\rho_{ik}(T, \mathbf{B}) = \rho_{ik}(T, 0) + \varepsilon_{ikl} \alpha_{lm}(T) B_m + \beta_{iklm}(T) B_l B_m \quad (3)$$

where  $\varepsilon_{ikl} = +1$  for  $i, k, l = 1, 2, 3$  (or any even permutation),  $\varepsilon_{ikl} = -1$  for odd permutations, and zero otherwise.

In a standard measurement of the electrical resistivity one determines the electrical field component along the current direction (say  $\mathbf{n}$ ), i. e.

$$\mathbf{E} \cdot \mathbf{n} = E_i n_i = \rho_{ik} n_i j_k \quad (4)$$

with  $\mathbf{j} = j \mathbf{n}$ ,  $|\mathbf{n}| = 1$ . We then have for the electrical resistivity measured at temperature  $T$ , in the  $\mathbf{n}$ -direction and under a magnetic induction  $\mathbf{B}$ :

$$\rho(T, \mathbf{n}, \mathbf{B}) = (\mathbf{E} \cdot \mathbf{n}) / j = \rho_{ik} n_i n_k \quad (5)$$

Introducing  $\rho_{ik}$  given by eq. (3), we obtain:

$$\begin{aligned} \rho(T, \mathbf{n}, \mathbf{B}) &= \rho_{ik}(T, 0) n_i n_k + [\varepsilon_{ikl} n_i n_k] \alpha_{lm}(T) B_m \\ &+ [\beta_{iklm}(T) n_i n_k] B_l B_m = \rho(T, \mathbf{n}, 0) + \lambda_{lm}(T, \mathbf{n}) B_l B_m \end{aligned} \quad (6)$$

where  $\lambda_{lm}(T, \mathbf{n}) = \beta_{iklm}(T) n_i n_k$ , and the first order terms in  $\mathbf{B}$  do not contribute to the electrical resistivity ( $\varepsilon_{ikl} n_i n_k = 0$ ).

We can then define a magnetoresistivity coefficient (eq. 1) corresponding to an electrical current along  $\mathbf{n}$  and a magnetic induction along  $\hat{\mathbf{b}}$  ( $\mathbf{B} = B \hat{\mathbf{b}}$ ,  $|\hat{\mathbf{b}}| = 1$ ):

$$\begin{aligned} (\Delta\rho/\rho)_{\mathbf{n}, \hat{\mathbf{b}}} &= [\rho(T, \mathbf{n}, \mathbf{B}) - \rho(T, \mathbf{n}, 0)] / \rho(T, \mathbf{n}, 0) \\ &= [\lambda_{lm}(T, \mathbf{n}) / \rho(T, \mathbf{n}, 0)] B_l B_m = [\gamma_{lm}(T, \mathbf{n}) \beta_l \beta_m] B^2 \end{aligned} \quad (7)$$

where

$$\gamma_{lm}(T, \mathbf{n}) \equiv \lambda_{lm}(T, \mathbf{n}) / \rho(T, \mathbf{n}, 0).$$

The quadratic field dependence of the magnetoresistivity, obtained at the present level of approximation, is well reproduced by the experimental result in most metallic systems investigated [1-3].

### Magnetic metals

In this case, because of the existence of magnetic moments  $\mathbf{m}_i$ , the curvature effect associated with the Lorentz force is enhanced, due to the increase of the internal magnetic induction:

$$\mathbf{B} = \mu_0 (\mathbf{H} + \mathbf{M} + \mathbf{H}_d) \quad (8)$$

$\mathbf{M}$  is the *technical* magnetization produced in the sample by the applied magnetic field,  $\mathbf{M} = \sum_i \langle \mathbf{m}_i \rangle / \Omega$  ( $\Omega$  is the sample volume), and  $\mathbf{H}_d$  is the demagnetizing field,  $\mathbf{H}_d = -D\mathbf{M}$  ( $D$  = demagnetizing factor; we assume, for simplicity, an ellipsoidal sample) [5, 18].

Besides the curvature effect, we must also consider carefully the scattering between the conduction electrons and the magnetic moments  $\mathbf{m}_i$ . The corresponding contribution to the electrical resistivity depends on the degree of magnetic order present in the sample, i. e. on the value of the spontaneous magnetization at each temperature,  $M_s(T)$  (mean field effect), and on the magnetic moment correlations e. g.  $\langle \mathbf{m}_i \cdot \mathbf{m}_j \rangle$ , particularly near the critical points (fluctuation effects) [19].

Furthermore, since each electron collision with a magnetic moment is in general anisotropic (angle  $\mathbf{k}$ ,  $\mathbf{m}_i$ ), the electrical resistivity also depends on the angle  $\theta$  between the electrical current and the technical magnetization  $\mathbf{M}$  (or, equivalently, of the applied field  $\mathbf{H}$ ) [5].

Putting these effects together (curvature, degree of magnetic order and scattering anisotropy) we can write:

$$\rho_{ik}(T, \mathbf{H}) = \rho_{ik}^0(T, \mathbf{B}) + \rho_{ik}^m(T, M_s, \theta, \langle \mathbf{m}_\alpha \cdot \mathbf{m}_\beta \rangle) \quad (9)$$

where  $\rho_{ik}^0$  contains the normal magnetoresistivity effect (with the trivial inclusion of  $\mathbf{M}$  effects in  $\mathbf{B}$ , eq. 8) and  $\rho_{ik}^m$  represents the new magnetic contributions, associated with magnetic order ( $M_s$  + correlations between fluctuations) and with the electron scattering anisotropy (angle  $\theta$ ).

In the following section we focus attention on some basic microscopic mechanisms which can contribute to the magnetoresistivity term  $\rho_{ik}^m$ . Within the scope of this paper, such treatment will be mainly illustrative rather than exhaustive.

## 2.2 — *Thermal disorder and fluctuation effects. Microscopic mechanisms in magnetic metals*

### a) Zero field case ( $\mathbf{H} = 0$ )

In a perfect crystal with the moments  $\mathbf{m}_i$  fully ordered at  $T = 0\text{K}$ , the conduction electrons travel through a periodic potential (electrostatic + magnetic), with no damping in the corresponding wavepackets; we then have  $\rho = 0$  (\*). In a simple

---

(\*) In an *ideally pure* crystal, no d. c. conductivity exists at  $T = 0\text{K}$ ; the conduction electrons simply oscillate under the action of a d. c. electrical field, due to the characteristic periodicity of the energy bands [20].

approximation the motion of a conduction electron through the lattice can be described by the Hamiltonian:

$$\mathcal{H} = -\hbar^2/(2m) \nabla^2 + \sum_{i=1}^N v(\mathbf{r} - \mathbf{R}_i) + \sum_{i=1}^N G(\mathbf{r} - \mathbf{R}_i) \mathbf{s} \cdot \mathbf{J}_i \quad (10)$$

where the first term represents the electron kinetic energy, the second term the electrostatic electron-lattice interaction ( $\mathbf{R}_i$  refers to the  $i$  ion in the lattice and  $\mathbf{r}$  to the electron position), and the third one gives the magnetic interaction between the electron spin  $\mathbf{s}$  and the ionic magnetic moment  $\mathbf{m}_i = (g_J - 1) \mu_B \mathbf{J}_i$  ( $g_J$  is the Landé factor and  $\mu_B$  is the Bohr magneton);  $\mathbf{J}_i$  is the total angular momentum of the ion  $i$  and  $G(\mathbf{r} - \mathbf{R}_i)$  measures the strength of the magnetic interaction.

At finite temperatures and below the Curie point (assuming, for simplicity, a ferromagnet), thermal disorder breaks the periodicities of the last term in eq. 10, with the consequent appearance of a magnetic resistivity contribution. Standard transport theory leads to the following expression for the magnetic resistivity measured along the  $i$  crystal direction [21, 22]:

$$\rho_m^{(i)}(T) / \rho_m^{(i)\infty} = \sum_{j=0}^N \Gamma(\mathbf{R}_j, T) \phi^{(i)}(\mathbf{R}_j) \quad (11)$$

where  $\rho_{m\infty}$  is the saturation value of the magnetic resistivity ( $T \gg T_c$ ),  $\Gamma(\mathbf{R}_j, T)$  is the correlation function between ionic moments at distance  $\mathbf{R}_j$ ,

$$\Gamma(\mathbf{R}_j, T) = \langle \mathbf{J}_0 \cdot \mathbf{J}_j \rangle / [J(J+1)] \quad (12)$$

and  $\phi^{(i)}(\mathbf{R}_j)$  is the interference function for the electron scattering from different ions, which has the electron wavelength  $\lambda_F$  as a characteristic parameter for each metal. For an arbitrary crystal lattice,  $\phi^{(i)}(\mathbf{R}_j)$  is generally anisotropic, always satisfying the two conditions:

$$\sum_{j=0}^N \phi^{(i)}(\mathbf{R}_j) = 0, \quad \phi^{(i)}(\mathbf{0}) = 1 \quad (13)$$

Notice also that  $\Gamma(\mathbf{0}, T) = 1$ .

Introducing these conditions in eq. 11 we obtain:

$$\frac{\rho_m^{(i)}(T)}{\rho_m^{(i)\infty}} = 1 + \sum_{j \neq 0}^N \frac{\langle \mathbf{J}_i \cdot \mathbf{J}_j \rangle}{J(J+1)} \phi^{(i)}(\mathbf{R}_j) \quad (14)$$

Using the angular momentum thermal averages  $\langle \mathbf{J}_i \rangle$ ,  $\langle \mathbf{J}_j \rangle$  and the thermal fluctuations  $\delta \mathbf{J}_i$ ,  $\delta \mathbf{J}_j$  we can write:

$$\mathbf{J}_i = \langle \mathbf{J}_i \rangle + \delta \mathbf{J}_i, \quad \mathbf{J}_j = \langle \mathbf{J}_j \rangle + \delta \mathbf{J}_j \quad (15)$$

and thus

$$\langle \mathbf{J}_i \cdot \mathbf{J}_j \rangle = \langle \mathbf{J}_i \rangle \cdot \langle \mathbf{J}_j \rangle + \langle \delta \mathbf{J}_i \cdot \delta \mathbf{J}_j \rangle \quad (16)$$

In a single domain ferromagnet,  $\langle \mathbf{J}_i \rangle = \langle \mathbf{J}_j \rangle = \langle \mathbf{J}^z \rangle \hat{\mathbf{z}}$  and  $\langle \mathbf{J}^z \rangle = J \sigma(T)$ , where  $\sigma(T)$  is the reduced spontaneous magnetization at temperature  $T$ ,  $\sigma(T) = M_s(T)/M_s(0)$ ; we then have

$$\langle \mathbf{J}_i \cdot \mathbf{J}_j \rangle = J^2 [\sigma(T)]^2 + \langle \delta \mathbf{J}_i \cdot \delta \mathbf{J}_j \rangle \quad (17)$$

Introducing these results in eq. 14, and using the properties of  $\phi^{(i)}(\mathbf{R}_j)$ , we obtain:

$$\frac{\rho_m^{(i)}(T)}{\rho_{m\infty}} = 1 - \frac{J}{J+1} [\sigma(T)]^2 + \frac{1}{J(J+1)} \sum_{i \neq 0}^N \langle \delta \mathbf{J}_i \cdot \delta \mathbf{J}_j \rangle \phi^{(i)}(\mathbf{R}_j) \quad (18)$$

The  $[\sigma(T)]^2$  term represents the mean field effect on  $\rho_m^{(i)}$ , associated with the temperature variation of the spontaneous magnetization. The last term gives the effect of the *correlations* between the thermal fluctuations in different ions.

If the system is not too close to the Curie point, the fluctuations  $\delta \mathbf{J}_i$  and  $\delta \mathbf{J}_j$  are usually fairly small and  $\rho_m^{(i)}(T)$  is dominated by the mean field term. Close to the Curie point  $\sigma(T) \rightarrow 0$ , the thermal fluctuations grow very rapidly, and the last term in eq. 18 may become important (\*). The correlations between the thermal fluctuations ( $\delta \mathbf{J}_i$  and  $\delta \mathbf{J}_j$ ) therefore determine the critical behaviour of the electrical resistivity near  $T_c$ .

For temperatures not in the immediate vicinity of  $T_c$ , the correlations between fluctuations can be described in terms of a mean field treatment (Landau type [16];  $|(T - T_c)/T_c| > \varepsilon_G$ , where  $\varepsilon_G$  is the so called reduced Ginzburg temperature [23], usually of the order of  $10^{-2}$  for many magnetic metals).

(\*) The fluctuations may be large, but if they are *uncorrelated*, the corresponding term  $\langle \delta \mathbf{J}_i \cdot \delta \mathbf{J}_j \rangle$  could still be neglected.

For temperatures in the range  $|(T - T_c)/T_c| < \epsilon_G$ , a full treatment of the fluctuations is necessary, within the context of the modern theories of critical phenomena [24], namely renormalization group treatments [25, 26]. Inside such critical region, scaling laws apply, and the critical exponents depend only on the lattice dimensionality ( $d$ ) and on the number of components ( $n$ ) of the order parameter; in particular, they are independent of the symmetry of the crystal lattice and of the direction in which the electrical resistivity is measured [27].

#### b) Magnetic field effects

When a magnetic field ( $\mathbf{H}$ ) is applied, two distinct effects arise, in connection with the terms discussed in eq. 18. First, the progressive alignment of the magnetic moments  $\mathbf{m}_i$  produced by  $\mathbf{H}$  increases the value of the sample magnetization, reducing therefore  $\rho_m(T)$  (negative magnetoresistance arising from the mean field term in eq. 18). Second, the field  $\mathbf{H}$  modifies the correlations between the different magnetic moments ( $i, j$ ), an effect which becomes increasingly important as  $T$  approaches  $T_c$ . This leads to characteristic critical features in the magnetoresistance near  $T_c$ , both in terms of the temperature and of the magnetic field. The sign of the corresponding magnetoresistance depends on the particular system under study, through the interplay between  $\phi^{(i)}(\mathbf{R}_j; \lambda_F)$  and  $\langle \delta \mathbf{J}_i \cdot \delta \mathbf{J}_j \rangle$ , in the lattice sum of eq. 18.

An extended summary of such effects of  $\mathbf{H}$  (on thermal disorder and fluctuations) has been given recently in the literature [13], including the critical indices theoretically expected for the magnetoresistivity in the vicinity of the Curie point, within different temperature and magnetic field ranges [6, 28, 29].

### 2.3 — Anisotropy of $\rho_m$ versus $\mathbf{M}_s$ ( $\mathbf{H} = 0$ )

#### 2.3.1 — Phenomenological approach

##### a) Single domain ferromagnetic crystal

Quite generally [30], the electrical resistivity of a single domain monocrystalline ferromagnetic metal, besides the dependence on the temperature due to spin disorder (section 2.2), also

depends on the direction of the electrical current  $\mathbf{l}$  with respect to the crystal axes  $\mathbf{c}_i$  (lattice anisotropy, e.g. due to different dynamical properties of the conduction electrons travelling along different crystal directions) and on the angle between  $\mathbf{l}$  and the spontaneous magnetization  $\mathbf{M}_s$  (magnetic anisotropy, e.g. due to spin-orbit effects on the scattering of the electrons by the ionic magnetic moments). Normally we can write [31]:

$$\rho(\hat{\mathbf{a}}, \hat{\mathbf{b}}) = F(\alpha_i, \beta_i, T) \quad (19)$$

where  $\alpha_i$  and  $\beta_i$  are the cosines of the angles ( $\mathbf{M}_s, \mathbf{c}_i$ ) and ( $\mathbf{l}, \mathbf{c}_i$ ) respectively (\*);  $\hat{\mathbf{a}}, \hat{\mathbf{b}}$  are the corresponding unit vectors.

The general form of  $F$  depends on the symmetry of the crystal under consideration, as it must be invariant with respect to all its symmetry operations. For example, in the case of hexagonal symmetry and to a fourth order approximation, one can show, in analogy with similar formulae for the magnetostriction [32] (a physical property with the same tensorial character as the electrical resistivity):

$$\rho(\hat{\mathbf{a}}, \hat{\mathbf{b}}) = a_0 + k_1(\beta_3^2 - 1/3) + k_2(\alpha_3^2 - 1/3) + k_3(\beta_3^2 - 1/3)(\alpha_3^2 - 1/3) + k_4[(\alpha_1^2 - \alpha_2^2)(\beta_1^2 - \beta_2^2) + 4\alpha_1\alpha_2\beta_1\beta_2] + k_5(\alpha_1\beta_1 + \alpha_2\beta_2)\alpha_3\beta_3 \quad (20)$$

where  $a_0$  is the non-orientational contribution to the resistivity (given in 2.2) and  $k_i$  are the anisotropy constants for the *electrical resistivity*.

#### b) Multidomain ferromagnetic crystal

The direction of the current with respect to the crystal axes continues to have a single value  $\hat{\mathbf{b}}$ . However, because of the domain magnetic structure, the direction of  $\mathbf{M}_s$  with respect to the crystal axes changes from one domain to the next. In each domain  $\mathbf{M}_s$  selects one of the ( $n$ ) easy directions in the crystal, which we characterize by the unit vector  $\hat{\mathbf{a}}_l$  ( $l = 1, 2, \dots, n$ ).

Since the orientational anisotropy of the resistivity is fairly small, the  $\rho$ -differences between different domains are small

---

(\*) We include explicitly the angles between  $\mathbf{M}_s$  and the crystal axes, since the crystal anisotropy is always operative, and may distinguish different directions of  $\mathbf{M}_s$  with respect to  $\mathbf{c}_i$ , e.g. through magnetoelastic effects.

compared with the domain resistivities  $\rho(\hat{\mathbf{a}}_l, \hat{\mathbf{b}})$ . The effective resistivity of such multidomain structure can then be approximated by [33],

$$\rho_{\text{ef}}(\hat{\mathbf{b}}) \simeq \left\{ \rho(\hat{\mathbf{a}}_l, \hat{\mathbf{b}}) \right\} \quad (21)$$

where  $\left\{ \dots \right\}$  means a spatial average over the sample, and a fine domain structure is assumed. We then write:

$$\rho_{\text{ef}}(\hat{\mathbf{b}}) \simeq (1/\Omega) \sum_{l=1}^n \sum_{r=1}^{N_d} c_{rl} \rho(\hat{\mathbf{a}}_l, \hat{\mathbf{b}}) \omega_d^{(r)} \quad (22)$$

where  $\Omega$  is the sample volume,  $\omega_d^{(r)}$  is the volume of the  $r$  magnetic domain ( $r = 1, 2, \dots, N_d$ ), and  $c_{rl}$  are occupation numbers:  $c_{rl} = 1$  if the domain  $r$  has  $\mathbf{M}_s$  along the  $l$  easy crystal direction, and  $c_{rl} = 0$  otherwise. A complete description of the domain structure means therefore the knowledge of all the individual domain volumes  $\omega_d^{(r)}$  and of the corresponding easy direction ( $c_{rl}$  coefficients).

Performing first the  $r$  sum we get,

$$\rho_{\text{ef}}(\hat{\mathbf{b}}) = (1/\Omega) \sum_{l=1}^n \rho(\hat{\mathbf{a}}_l, \hat{\mathbf{b}}) \sum_{r=1}^{N_d} c_{rl} \omega_d^{(r)} \quad (23)$$

Notice that  $\sum_{r=1}^{N_d} c_{rl} \omega_d^{(r)}$  gives the total domain volume corresponding to the  $l$  orientation, which we call  $\omega_d(l)$ ; we then have

$$\rho_{\text{ef}}(\hat{\mathbf{b}}) = (1/\Omega) \sum_{l=1}^n \rho(\hat{\mathbf{a}}_l, \hat{\mathbf{b}}) \omega_d(l) \quad (24)$$

If the magnetic domains are equally distributed over the easy directions,  $\omega_d(l) = \Omega/n$ ; and the simple result appears:

$$\rho_{\text{ef}}(\hat{\mathbf{b}}) = (1/n) \sum_{l=1}^n \rho(\hat{\mathbf{a}}_l, \hat{\mathbf{b}}) \quad (25)$$

### c) Multidomain polycrystalline ferromagnet

We assume the sample as an assembly of  $N_c$  crystallites oriented at random, each one numbered by an index  $j$ , with volume  $\Omega_j$ , and with its own magnetic domain structure. Due to the polycrystalline structure, the current  $\mathbf{I}$  makes in general different angles  $(\mathbf{I}, \mathbf{c}_1^{(j)})$  with the crystal axes of the different

crystallites,  $\mathbf{c}_i^{(j)}$ . The direction of  $\mathbf{l}$  inside each crystallite can then be associated with a corresponding unit vector  $\hat{\mathbf{b}}^{(j)}$ . Due to the domain structure, we can first calculate the effective resistivity of each crystallite, using eq. 24:

$$\rho_{\text{ef}}(\hat{\mathbf{b}}^{(j)}) = (1 / \Omega_j) \sum_{l=1}^n \rho(\hat{\mathbf{a}}_l, \hat{\mathbf{b}}^{(j)}) \omega_d^{(j)}(l) \quad (26)$$

The spatial average over the crystallites can now be written:

$$\rho_{\text{ef}}(\text{sample}) = (1 / \Omega) \sum_{j=1}^{N_c} \rho_{\text{ef}}(\hat{\mathbf{b}}^{(j)}) \Omega_j \quad (27)$$

Introducing the explicit form of  $\rho_{\text{ef}}(\hat{\mathbf{b}}^{(j)})$ , eq. 26, we obtain:

$$\rho_{\text{ef}}(\text{sample}) = (1 / \Omega) \sum_{j=1}^{N_c} \sum_{l=1}^n \rho(\hat{\mathbf{a}}_l, \hat{\mathbf{b}}^{(j)}) \omega_d^{(j)}(l) \quad (28)$$

If we assume that the crystallites have similar volumes ( $\Omega_j \approx \Omega / N_c$ ) and that  $\mathbf{M}_s$  is equally distributed over the  $n$  easy directions, we then get the simple result:

$$\rho_{\text{ef}}(\text{sample}) = 1 / (N_c n) \cdot \sum_{j=1}^{N_c} \sum_{l=1}^n \rho(\hat{\mathbf{a}}_l, \hat{\mathbf{b}}^{(j)}) \quad (29)$$

### 2.3.2 — Microscopic approach

Physical origin of the  $(\mathbf{l}, \mathbf{M}_s)$  anisotropy; Smit mechanism.

Experiment shows that the anisotropy of the electrical resistivity with respect to the direction of the spontaneous magnetization,  $\mathbf{M}_s$ , is present in most magnetic metals, ranging from heavy rare earths [12, 34] to 3d transition elements [5] (localized, quasi-localized or itinerant magnetism), either isolated or in the form of alloys, compounds or pseudocompound systems. Furthermore, the anisotropy is present even in the cases when the crystal lattice has cubic symmetry. This shows that the observed anisotropy has a magnetic origin, and must be a consequence of an anisotropic scattering mechanism. In the case of cubic crystals, the anisotropy could result from some lower-than-cubic-symmetry scattering potential (e. g. magnons) with cubic-symmetry initial and final states, or from an isotropic scattering potential with lower-than-cubic-

symmetry wavefunctions [30, 35, 36, 37]. The latter mechanism is generally considered the more likely one in the case of 3d transition metals, and was successfully applied, for the first time, by Smit [4] to discuss the intriguing resistivity anisotropy in cubic transition metal ferromagnets. To illustrate the subtle mechanisms underlying the magnetic anisotropy, we will concentrate here only on the Smit mechanism, following closely the review of McGuire and Potter [30], which assumes an isotropic scattering potential  $V(r)$ .

As observed by Smit, in 3d cubic crystals the symmetry of the electronic wavefunctions associated with each lattice ion can be lowered by the spin-orbit interaction,

$$H_{so} = k \mathbf{L} \cdot \mathbf{S} \quad (30)$$

provided the electrostatic potential is radial;  $\mathbf{L}$  and  $\mathbf{S}$  are the ion total orbital momentum and total spin, respectively, whereas  $k$  measures the strength of the spin-orbit coupling.

In the absence of such interaction, the five 3d atomic orbitals are degenerate ( $\varphi_1 = xzf(r)$ ,  $\varphi_2 = yzf(r)$ ,  $\varphi_3 = xyf(r)$ ,  $\varphi_4 = (x^2 - y^2)f(r)/2$ ,  $\varphi_5 = (r^2 - 3z^2)f(r)/(2\sqrt{3})$ ), and such degeneracy remains even when we switch the (cubic symmetry) crystal field interaction. Recalling that in transition metals the main resistivity mechanism results from the transitions of electrons from the s-conduction band ( $\psi_s \sim e^{ik \cdot r}$ ; high mobility; low effective mass) to the d-band ( $\Phi_i$  wavefunctions; appropriate linear combinations of  $\varphi_i$  functions, with the crystal field (cubic) symmetry; low mobility; high effective mass), no anisotropy exists in the absence of spin-orbit coupling (within the model under discussion).

The spin-orbit interaction makes a contribution to the energy of the d-states that depends on spin or magnetization direction, making it favourable for  $\mathbf{M}_s$  to point along certain crystallographic directions. Thus the d-electron spin is coupled to its orbital motion, which in turn is coupled to the lattice by the crystal field. In the presence of  $H_{so}$ , the degeneracy in the  $\Phi_i$  functions is lifted, and new wavefunctions  $\Phi_i^{(1)}$  then result, associated with each 3d ion. Due to the direction effect of  $\mathbf{M}_s$ , the functions  $\Phi_i^{(1)}$  exhibit symmetry lower than cubic and are not eigenfunctions of  $S_z$  because  $H_{so}$  mixes states of opposite spin.

Because the levels associated with different  $\Phi_i^{(1)}$  functions have not all the same energy, a particular combination of  $\varphi_i$  functions is therefore energetically favoured. If some functions  $\varphi_i$  predomi-

nate over the others in such particular combination, the resistivity anisotropy immediately results. To illustrate this in simple terms, let us choose an extreme case in which the spin-orbit interaction selects, as dominant, the function  $\varphi_3 = xyf(r)$  (in this case,  $\mathbf{M}_s$  points along OZ, by symmetry).

The transition probability of a conduction electron ( $\mathbf{k}$  vector,  $\psi_{\mathbf{k}} \sim e^{i\mathbf{k}\cdot\mathbf{r}}$ ) to the 3d band ( $\varphi_3$  state), produced by the scattering potential  $V(r)$ , is proportional to the usual Born approximation factor,

$$P_{sd}(\psi_{\mathbf{k}} \rightarrow \varphi_3) \propto \left| \int e^{-i\mathbf{k}\cdot\mathbf{r}} V(r) \varphi_3 d^3 r \right|^2 \quad (31)$$

Since  $k_F \approx a^{-1}$  ( $a =$  atomic spacing) and  $\varphi_3$  is localized in the vicinity of the scattering ion, the dominant contributions to the integral correspond to  $|\mathbf{k}\cdot\mathbf{r}| \ll 1$ , which justifies a series development of the exponential. We then have, after trivial calculations,

$$P_{sd}(\psi_{\mathbf{k}} \rightarrow \varphi_3) \propto k_x^2 k_y^2 \left| \int (xy)^2 V(r) f(r) d^3 r \right|^2 \quad (32)$$

The s-d transition probability is in this case highly anisotropic,  $P_{sd} \propto k_x^2 k_y^2$ , depending on the particular direction of the electron ( $\mathbf{k}$ ). For example, for an electron moving along OX or OY ( $k_y = 0$ ,  $k_x = 0$ , respectively) no scattering occurs, whereas collisions occur when both  $k_x$  and  $k_y$  are different from zero. We recall that the reference axes have been imposed by the  $\mathbf{M}_s$  direction, along OZ in the particular case just discussed. Therefore, the anisotropy with respect to the crystal axes is primarily due to the anisotropy with respect to  $\mathbf{M}_s$ .

#### 2.4 — Anisotropy of $\rho_m$ v. technical magnetization $\mathbf{M}$ ( $H \neq 0$ )

##### 2.4.1 — General expressions

For the general case of a polycrystalline ( $N_c$  crystallites) multidomain ferromagnet we have seen that the zero field electrical resistivity is given by the expression,

$$\rho_{ef}(T, 0) = (1/\Omega) \sum_{j=1}^{N_c} \sum_{l=1}^n \rho(\hat{\mathbf{a}}_j, \hat{\mathbf{b}}^{(j)}) \omega_d^{(j)}(l, 0) \quad (33)$$

where  $\omega_d^{(j)}(l, 0)$  represents the total volume of the domains in crystallite  $j$  orientated along the  $l$ -easy direction (for  $\mathbf{H} = 0$ ).

When a magnetic field is applied, the first effect is a redistribution of the domain pattern, through domain wall motion, so as to increase the domains oriented in favourable directions (with respect to  $\mathbf{H}$ ) at the expense of the domains oriented in unfavourable directions. Provided no magnetic domain is extinct in such initial process, the sum over  $l$  is still complete, and the only field effect will be the change in the individual magnetic domains. We can then write for the corresponding magnetoresistivity:

$$\left(\frac{\Delta\rho}{\rho}\right)_{\text{wall motion}} = \frac{1}{\rho(T, 0)} \cdot \frac{1}{\Omega} \sum_{j=1}^{N_c} \sum_{l=1}^n \rho(\hat{\mathbf{a}}_l, \hat{\mathbf{b}}^{(j)}) \Delta\omega_d^{(j)}(l, \mathbf{H}) \quad (34)$$

where  $\Delta\omega_d^{(j)}(l, \mathbf{H}) = \omega_d^{(j)}(l, \mathbf{H}) - \omega_d^{(j)}(l, 0)$ .

When some of the easy directions cease to be represented by magnetic domains, the sum over  $l$  is progressively restricted. Ultimately, at higher fields, only a single easy direction survives in each crystallite (monodomain situation), not necessarily the same for all crystallites. Representing such particular crystallite easy direction by a unit vector  $\hat{\mathbf{a}}_{l_j}$ , we then have:

$$\rho_{\text{ef}}(T, \mathbf{H}) = \frac{1}{\Omega} \sum_{j=1}^{N_c} \sum_{l=1}^n \rho(\mathbf{a}_l, \mathbf{b}^{(j)}) \omega_d^{(j)}(l, \mathbf{H}) \delta_{l, l_j} \quad (35)$$

When the field produces this situation, no further domain wall motion exists inside each crystallite, and the magnetization process can only proceed through *rotation* of the spontaneous magnetization inside each crystallite, towards progressive alignment with the magnetic field  $\mathbf{H}$ .

The above expressions, although physically adequate to identify the various effects associated with the magnetoresistive process, are not in a simple form appropriate to analyze the experimental results. Such formulae can be obtained through an adequate averaging process over the sample, restricted to the case of saturation resistivity, i. e.  $\Delta\rho$  is calculated between an initial demagnetized state (random domain distribution) and a final state where  $\mathbf{M}_s$  is everywhere aligned with  $\mathbf{H}$ .

As shown in next section, the following general expression is obtained for the orientational dependence of the magneto-resistivity,

$$(\Delta\rho/\rho)_{\text{sat}} = A(T) + B(T) \cos^2 \theta \quad (36)$$

where  $\theta$  is the angle between the electric current and  $\mathbf{H}$ , and  $A, B$  are temperature dependent quantities, which can be related with the magneto-resistivity anisotropy coefficients  $k_i$  (defined in 2.3.1.a)).

#### 2.4.2 — Averaging processes

##### (i) *Single crystal samples*

To illustrate this averaging process, let us take a hexagonal single crystal, with the electric current flowing along  $\hat{\mathbf{b}}$ .

When the applied field  $\mathbf{H}$  (along an  $\hat{\mathbf{u}}$  direction) produces magnetic saturation, we have  $\mathbf{M}_s \parallel \mathbf{H}$  everywhere in the sample, i. e.  $\hat{\mathbf{a}} = \hat{\mathbf{u}}$ . We can then calculate the saturation resistivity,  $\rho_{\text{sat}}$ , using eq. 20 for single crystals,

$$\rho_{\text{sat}} = \rho(\hat{\mathbf{u}}, \hat{\mathbf{b}}) = a_0 + k_1(\beta_3^2 - 1/3) + k_2(u_3^2 - 1/3) + k_3(\beta_3^2 - 1/3)(u_3^2 - 1/3) + k_4[(u_1^2 - u_2^2)(\beta_1^2 - \beta_2^2) + 4u_1u_2\beta_1\beta_2] + k_5(u_1\beta_1 + u_2\beta_2)u_3\beta_3 \quad (37)$$

When  $\mathbf{H} = 0$ , we assume the sample to be fully demagnetized, with the magnetic domains equally distributed over the easy directions. The result of the necessary averaging process depends on the particular easy directions imposed by the magnetic anisotropy of the sample. For example, if we have a basal plane ferromagnet, the easy directions lie entirely in this plane and we can take  $\alpha_1, \alpha_2 \neq 0, \alpha_3 = 0$  (taking the c-axis along  $\text{Ox}_3$ ). For this case we have the following zero field *domain* resistivity,

$$\rho(\hat{\mathbf{a}}, \hat{\mathbf{b}}) = (a_0 - k_2/3) + k_1(\beta_3^2 - 1/3) - 1/3 k_3(\beta_3^2 - 1/3) + k_4[(\alpha_1^2 - \alpha_2^2)(\beta_1^2 - \beta_2^2) + 4\alpha_1\alpha_2\beta_1\beta_2] \quad (38)$$

Because the domains are assumed equally distributed in the basal plane easy directions, when we average  $\rho$  over such directions we obtain a simple result (using  $\langle \alpha_1^2 \rangle = \langle \alpha_2^2 \rangle, \langle \alpha_1\alpha_2 \rangle = 0$ ):

$$\langle \rho(\hat{\mathbf{a}}, \hat{\mathbf{b}}) \rangle_{\mathbf{H}=0} = (a_0 - k_2/3) + (k_1 - k_3/3)(\beta_3^2 - 1/3) \quad (39)$$

The non-normalized saturation magnetoresistivity is then given by,

$$\Delta\rho_{\text{sat}}(\mathbf{H} \parallel \mathbf{u}) = \rho_{\text{sat}} - \langle \rho(\hat{\mathbf{a}}, \hat{\mathbf{b}}) \rangle_0 = k_2 u_3^2 + k_3 (\beta_3^2 - 1/3) u_3^2 + k_4 [(u_1^2 - u_2^2)(\beta_1^2 - \beta_2^2) + 4 u_1 u_2 \beta_1 \beta_2] + k_5 (u_1 \beta_1 + u_2 \beta_2) u_3 \beta_3 \quad (40)$$

If  $\mathbf{H}$  is applied along the c-axis ( $u_1 = u_2 = 0, u_3 = 1$ ) we obtain:

$$\Delta\rho_{\text{sat}}(\mathbf{H} \parallel \mathbf{c}) = (k_2 - k_3/3) + k_3 \beta_3^2 \quad (41)$$

Noticing that  $\beta_3$  is, in this case, the cosine of the angle ( $\theta$ ) between  $\mathbf{l}$  and  $\mathbf{H}$ , we arrive at eq. 36, in the explicit form:

$$\Delta\rho_{\text{sat}}(\mathbf{H} \parallel \mathbf{c}) = (k_2 - k_3/3) + k_3 \cos^2 \theta \quad (42)$$

### (ii) *Polycrystalline samples*

For this case we have to calculate an average of  $\rho(\hat{\mathbf{a}}, \hat{\mathbf{b}})$  over a large number of randomly oriented crystallites. Following McGuire and Potter [30], the polycrystalline average can be performed by choosing  $\hat{\mathbf{a}}$  to lie within a cone about an arbitrary current direction  $\hat{\mathbf{b}}$ , with  $\hat{\mathbf{a}} \cdot \hat{\mathbf{b}} = \cos \theta$ , and evaluating

$$\rho_{\text{poly}} = (8\pi^2)^{-1} \int_0^{2\pi} d\psi \int_0^\pi d\gamma \int_0^{2\pi} \rho(\hat{\mathbf{a}}, \hat{\mathbf{b}}) d\phi \quad (43)$$

where  $\psi$  is an angle that locates  $\hat{\mathbf{a}}$  within the cone as shown in Fig. 1. The final result gives again an expression with a  $\cos^2 \theta$  dependence for the magnetoresistivity (eq. 36).

## 3 — HIGH ACCURACY METHOD FOR MAGNETORESISTANCE MEASUREMENTS

### 3.1 — *Requirements on the experimental resolution*

As referred in 1, the magnetoresistive effects are fairly small, the relative change  $\Delta\rho/\rho$  under an applied magnetic field rarely attaining a value of  $10^{-2}$  at saturation. If we want to measure such magnetoresistivity with a relative error of 1%, one should have

$$\frac{\delta(\Delta\rho/\rho)}{\Delta\rho/\rho} = \frac{\delta(\Delta\rho)}{\Delta\rho} = \frac{\delta\rho}{\Delta\rho} = 10^{-2} \quad (44)$$

where  $\delta$  stands for the *absolute* errors. Putting  $\Delta\rho = 10^{-2}\rho$ , we obtain the following requirement on the *relative* accuracy for resistivity measurements,

$$\delta\rho/\rho = 10^{-4} \quad (45)$$

This estimate refers to the (favourable) measurement of  $\Delta\rho$  at the maximum field. If we want to study in detail the structure of

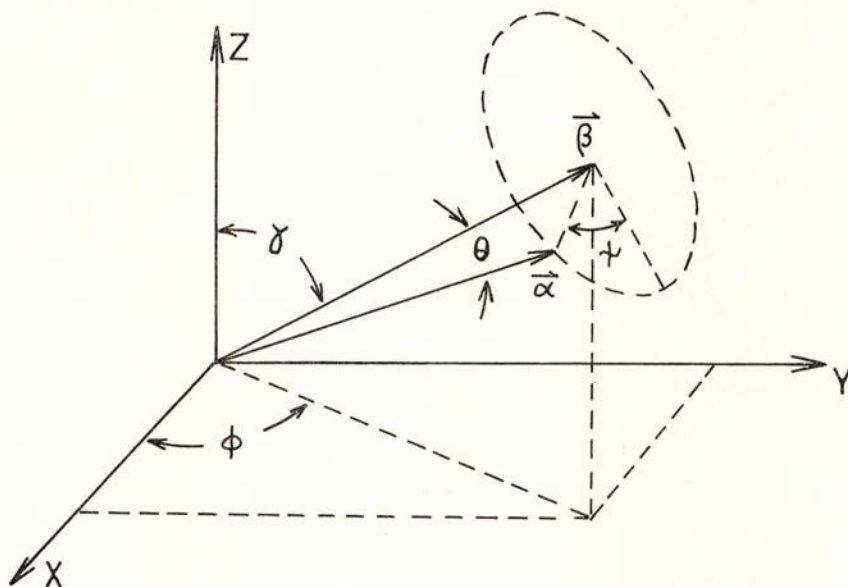


Fig. 1 — Geometry and notation used to calculate the polycrystalline average of the magneto-resistivity (eq. 43).

the magneto-resistivity curves (at field values from 0 to  $H_m$ ) one should measure the resistivity with higher resolution, at least one or two orders of magnitude better. We then conclude that high accuracy magneto-resistivity measurements require an experimental set-up which ensures, with confidence,  $1/10^5 - 1/10^6$  relative resolution in resistivity. The method here described fulfills this requirement.

### 3.2 — *Experimental technique*

The electrical resistivity, thus the magneto-resistivity, was measured with a four-wire potentiometric method, using a highly

stabilized dc current (0 - 1 A;  $1/10^6$  stability per hour), the sample voltage (V) being measured with a few nV resolution ( $V \sim 10^3 \mu\text{V}$ ).

The sample resistivity ( $\rho$ ) is given by the usual expression,

$$\rho = f \cdot (V/I) \quad (46)$$

where  $f$  is a constant geometric factor.

Under *strictly isothermal* conditions, we then have the following limit for the relative error in  $\rho$ :

$$|\delta\rho/\rho| \leq |\delta V/V| + |\delta I/I| \quad (47)$$

From the figures quoted above for  $\delta V/V$  and  $\delta I/I$ , we just obtain the appropriate resolution in the  $\rho$  measurements.

In practice the temperature is not strictly constant in the course of the measurement, when the field is gradually swepted from 0 to  $H_m$ ; usually a complete measuring cycle lasts for about 2-3 min. One should then ensure that the change in resistivity ( $\delta\rho_T$ ) due to a change in temperature during the measurement ( $\delta T$ ) is kept within the required limits. If one recalls that in most metals the relative changes in  $\rho$ , per degree change of temperature, are of the order of  $10^{-3}$  (or below), we can write

$$\delta\rho_T / \rho \approx 10^{-3} \delta T \quad (48)$$

which restricts the allowed temperature variation during the measuring process to a maximum value  $\delta T_{\text{max}} \approx 1$  mK, for  $\delta\rho_T / \rho \approx 10^{-6}$ . One then concludes that, in order to measure accurately the magnetoresistivity, it is crucial to implement an efficient temperature controller; such unit was projected and implemented in the course of our studies, and will be described in 3.3.

Fig. 2 shows the block diagram of the experimental set-up constructed to measure the magnetoresistivity.

The temperature was measured using a copper-constantan thermocouple, the corresponding emf being measured to within a few nV.

The low magnetic fields were obtained with a copper wire solenoid locally constructed [38] ( $0 \leq H \leq 1$  kOe;  $1:10^4$  homogeneity over 10 cm axial length), powered from a stabilized dc current supply ( $1:10^4$  stability). The solenoid calibration is

263 Oe/A. The solenoid is refrigerated with a water cooled coil, the ensemble being immersed in a large capacity oil bath.

The high fields ( up to 10 kOe ) are obtained with a commercial iron core electromagnet with an adjustable gap. The current is provided by a stabilized power supply ( 0-30 A ) with  $1:10^5$  stability.

In each case the field was automatically increased from 0 to  $H_m$  by means of a ramp sweep unit, which controlled the output of the magnet current supply (rising times adjustable between 10 s and 80 h; usually we adopted about 2 min).

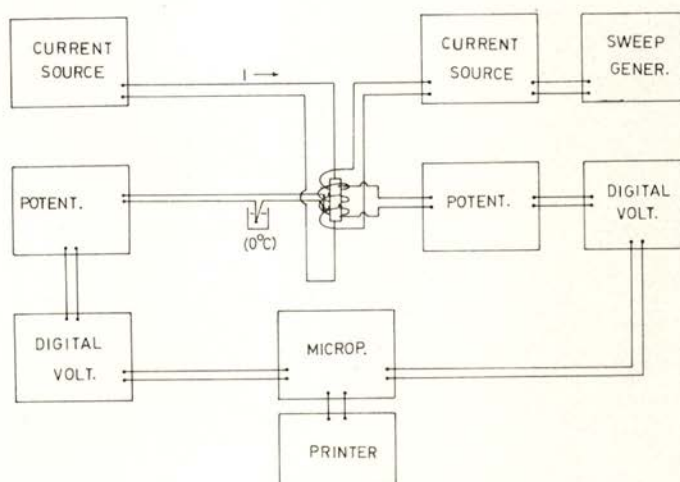


Fig. 2 — Block diagram of the experimental unit for magnetoresistivity measurements.

Automatic data acquisition was obtained with a microprocessor unit locally constructed [39], which prints the relevant data ( $\rho$ ,  $H$ ,  $T$ ) every 2 seconds, if necessary.

### 3.3 — *Temperature controller*

In order to ensure the necessary stability in temperature, an automatic temperature controller was designed, using a high precision digital lock'in phase sensitive detector. Fig. 3 shows the block diagram of such temperature controller.

The lock'in internal oscillator provides, besides the internal reference signal, the excitation voltage for the Wheatstone bridge. In two adjacent arms we use fixed resistances of  $200\ \Omega$ , whereas in the other arms we put the controller resistance thermometer (thin copper coil;  $r \approx 200\ \Omega$  at room temperature, about  $60\ \Omega$  at nitrogen temperatures) and a 4 decade resistance box with  $0.1\ \Omega$  resolution.

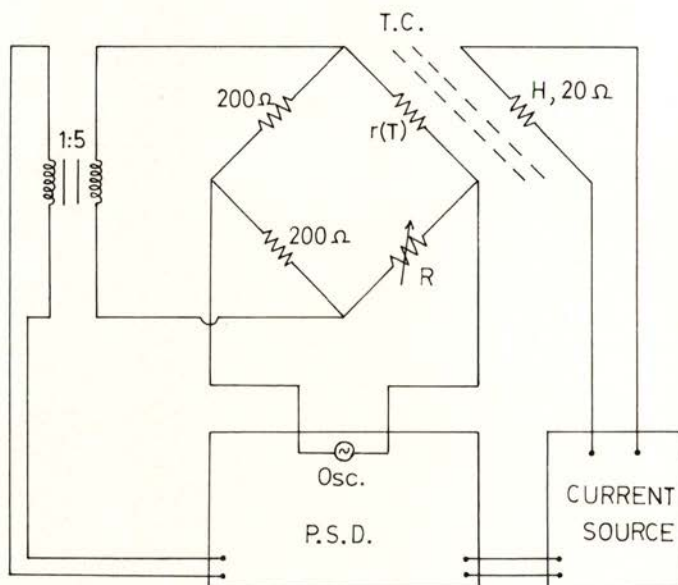


Fig. 3 — Block diagram of the temperature controller for magnetoresistivity measurements.

The unbalance signal from the bridge is accurately detected by the lock'in detector and, after suitable internal amplification, is used as the input of an unidirectional power supply. This source provides the current for the controlling heater of the experimental chamber ( $R \approx 20\ \Omega$ ; 5 W maximum heating power).

This temperature controller enables quick temperature adjustments (e. g. a 10 K variation in the setting point can be achieved in 5 min), with a guaranteed subsequent stability better than  $1\ \text{mK}/\text{min}$ . In order to ensure such degree of efficiency,

adequate attention has been paid to the design of the experimental chamber and the sample holder, as we describe next.

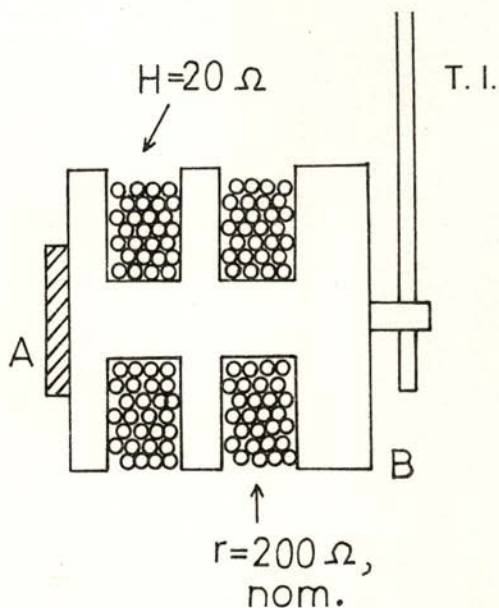


Fig. 4 — Details of the sample holder: A-sample, B-copper basis, H-heater, r-resistance thermometer, T. I.-inox tube.

### 3.4 — *Sample holder (and controller basis)*

In order to optimize all the thermal links in the system "sample-controller thermometer-heating coil", a special design was adopted for the supporting copper basis, as shown in Fig. 4. The coils of the controller copper thermometer and of the heater (constantan) are wound in narrow flat grooves in the immediate vicinity of the copper basis where the sample is attached with low temperature, thermal conducting, GE varnish. The ensemble is suspended inside the experimental chamber by two thin wall inox tubes, in order to increase the thermal resistance between the controlling copper basis and the external environment.

A limited account of the method described in this section has been given elsewhere [40].

#### 4 — ILLUSTRATIVE EXPERIMENTAL RESULTS

Experimentally, two distinct field orientations are usually adopted in magnetoresistivity measurements, either with the magnetic field perpendicular to the electrical current (Fig. 5a),

$$\Delta\rho_{\perp} / \rho = [\rho_{\perp}(T, H) - \rho(T, 0)] / \rho(T, 0) \quad (49)$$

or with  $\mathbf{H}$  parallel to  $\mathbf{I}$  (Fig. 5b),

$$\Delta\rho_{\parallel} / \rho = [\rho_{\parallel}(T, H) - \rho(T, 0)] / \rho(T, 0) \quad (50)$$

Here  $\rho(T, 0)$  is the sample resistivity in zero field.

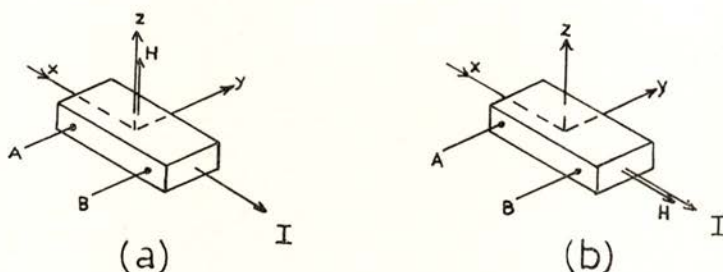


Fig. 5 — Distinct field orientations used for magnetoresistivity measurements:  
a) Transverse  $\Delta\rho_{\perp} / \rho$ , b) longitudinal  $\Delta\rho_{\parallel} / \rho$

In order to eliminate from  $\Delta\rho/\rho$  spurious odd effects in  $\mathbf{H}$ , we should always take the average, for each  $T$ , of the results obtained with the two opposite directions of the field ( $\pm \mathbf{H}$ ).

The results shown below illustrate some of the potentialities of the experimental method described in 3 and, at the same time, constitute selected examples of the behaviour of the magnetoresistivity contributions theoretically described in section 2.

#### 4.1 — *Critical phenomena* (ferro-paramagnetic transition in $\text{Tb}_{68} - \text{Gd}_{32}$ single crystal).

Fig. 6 shows the temperature dependence of the longitudinal magnetoresistivity of an hcp single crystal  $\text{Tb}_{68} - \text{Gd}_{32}$  (current  $\mathbf{I}$  in the basal plane) in the vicinity of the Curie point,  $T_c = 253$  K, and at a constant applied field  $H = 526$  Oe.

A pronounced negative dip occurs in  $\Delta\rho_{\parallel}/\rho$  just at the Curie point, which we associate with the characteristic strong reduction (by the field) of the spin fluctuations near a ferro-paramagnetic transition, as discussed in 2.2. Notice that both sides of the  $\Delta\rho_{\parallel}/\rho$  curve exhibit critical behaviour near  $T_c$ ; a full analysis of such behaviour, with the estimation of the corresponding critical exponents, will be done in due course.

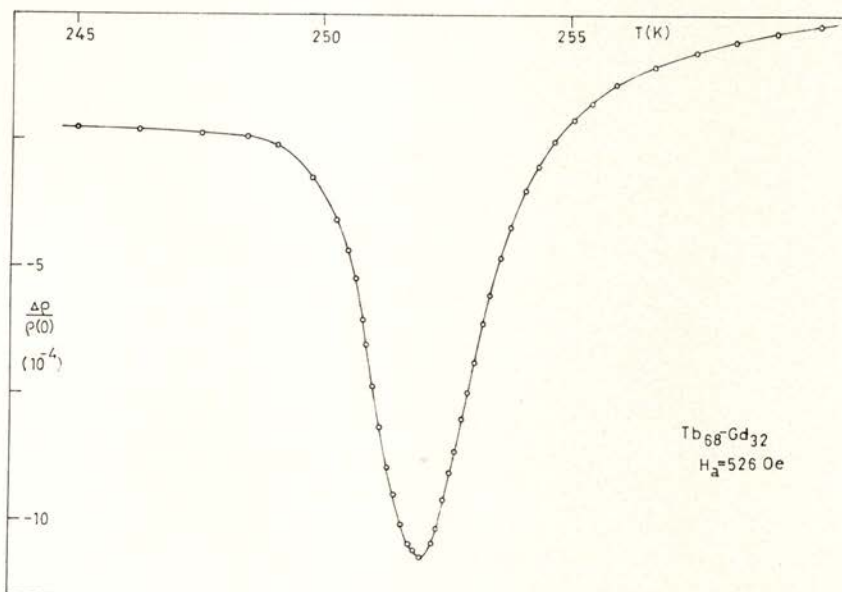


Fig. 6 — Temperature dependence of the longitudinal magnetoresistivity in a Tb<sub>68</sub> - Gd<sub>32</sub> single crystal.

Notice also that sufficiently above  $T_c$  (when the correlations between fluctuations are virtually absent), the magnetoresistivity is fairly small, attributable to just the non-magnetic (normal) magnetoresistivity.

On the other hand, for temperatures sufficiently below  $T_c$  the magnetoresistivity exhibits an almost constant negative value. Since fluctuations are then drastically damped, such result is attributed to an orientational effect of  $\mathbf{H}$  on the basal plane spontaneous magnetization, for which the low magnetic anisotropy readily enables directional changes in  $\mathbf{M}_s$ .

4.2 — *Orientalional effects* ( $\text{Pr}_2(\text{Co}_{1-x}\text{Fe}_x)_{17}$  intermetallic compounds)

Fig. 7 shows the field dependence of the longitudinal magneto-resistivity ( $H = 0 - 9.7 \text{ kOe}$ ) for a  $\text{Pr}_2(\text{Co}_{0.8}\text{Fe}_{0.2})_{17}$  polycrystalline sample ( $\text{Th}_2\text{Ni}_{17}$  hexagonal structure), at different values of the

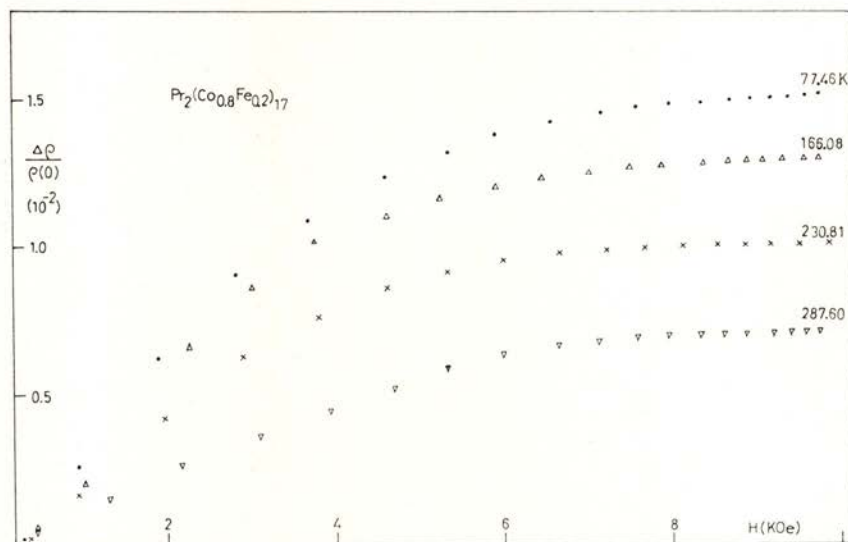


Fig. 7 — Field dependence of the longitudinal magneto-resistivity of a  $\text{Pr}_2(\text{Co}_{0.8}\text{Fe}_{0.2})_{17}$  polycrystalline sample, at several constant temperatures.

measuring temperature, with the sample always in the ferromagnetic phase ( $T \ll T_c$ ). The magneto-resistance is now positive, and entirely attributed to an orientational effect (Smit mechanism [5, 36, 37]; see 2.3.2).

In all the isothermal  $\Delta\rho_{\parallel}/\rho$  curves shown in Fig. 7, we distinguish three distinct regions, underlying characteristic dominant effects. In the first portion, at low fields, the curvature is positive and is associated with the growth of domains in favourable directions, at the expense of decreasing domains in unfavourable directions (wall domain motion). The second portion of the curve, with a noticeable negative curvature, is associated with the rotation of the magnetic domains inside the sample (towards the direction of  $H$ ), a process which is particularly difficult for those crystallites

where  $\mathbf{H}$  points in hard magnetic directions. Finally, a third region, at high fields (where saturation is almost achieved in  $\Delta\rho_{\parallel}/\rho$ ), is the final alignment stage of  $\mathbf{M}_s$  with  $\mathbf{H}$  (\*).

#### 4.3 — *Field effects on helimagnetic structures (Gd<sub>1-x</sub>-Y<sub>x</sub> single crystal)*

Fig. 8 shows the field dependence of the longitudinal magnetoresistivity ( $H = 0-520$  Oe) for a hcp Gd<sub>0.68</sub>-Y<sub>0.32</sub> single crystal ( $\mathbf{l} // \mathbf{c}$  axis) at several measuring temperatures, corresponding either to the ferro or to the helimagnetic phase, in zero field.

The crystal under investigation is ferromagnetic just above  $T_c^* = 208.15$  K, with  $\mathbf{M}_s$  along the  $\mathbf{c}$ -axis, and helimagnetic just below this temperature. In the latter phase the magnetic moments lie in the basal plane (ferromagnetically ordered), exhibiting however an helical modulation along the  $\mathbf{c}$ -axis, associated to a characteristic  $\mathbf{q}$  vector [42, 43].

(i) Let us start with the curve taken with the sample initially in the ferromagnetic phase ( $T = 208.55$  K).

At low fields ( $H \lesssim 50$  Oe), no measurable change is detected in  $\rho$ , a fact which we associate with the absence of field penetration in the sample. This is achieved by domain motion (\*\*), so as to produce a technical magnetization  $\mathbf{M} = \mathbf{H} / D$  in the sample, which ensures a zero value for the internal magnetic field,  $H_i = \mathbf{H} - D\mathbf{M}$ . An estimate of the maximum value of  $H$  compatible with the absence of field penetration,  $H_{\max} = DM_s(T)$  (using information on  $M_s(T)$  and  $D$  for our sample) confirms the explanation referred above.

At higher fields we observe a progressive reduction of the electrical resistivity, up to the maximum field used. This is attributed to the gradual suppression of the spin fluctuations, since the measuring temperature is only about 2 K below the Curie point of this crystal.

(\*) In practice, the *total* alignment of the magnetic moments with  $\mathbf{H}$  is not exactly achieved under finite fields, except for the principal symmetry directions in the crystal [41].

(\*\*) In uniaxial ferromagnets, the growth of domains of one type ( $+z$ ), at the expenses of the other type ( $-z$ ), does not change  $\rho$  (even function of  $\cos\theta$ ).

(ii) For the other curves, obtained with the crystal initially in the helimagnetic phase, the field penetration occurs immediately

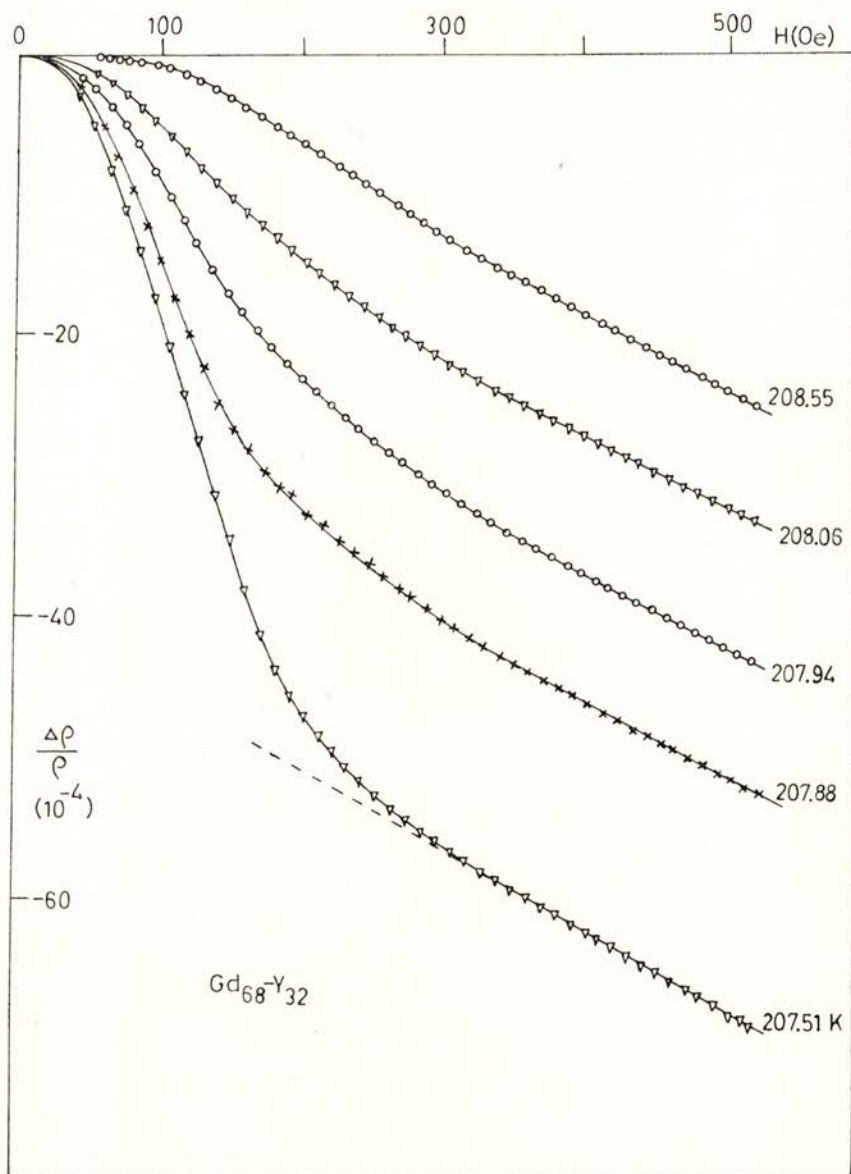


Fig. 8 — Field dependence of the longitudinal magneto-resistivity of a  $Gd_{0.68} - Y_{0.32}$  single crystal, with  $I \parallel c$  axis, at several constant temperatures.

at low fields, as expected for an antiferromagnetic structure [44].

A pronounced negative magneto-resistance is first observed in the  $\Delta \rho_{\parallel} / \rho$  curve, as a result of the gradual distortion of the

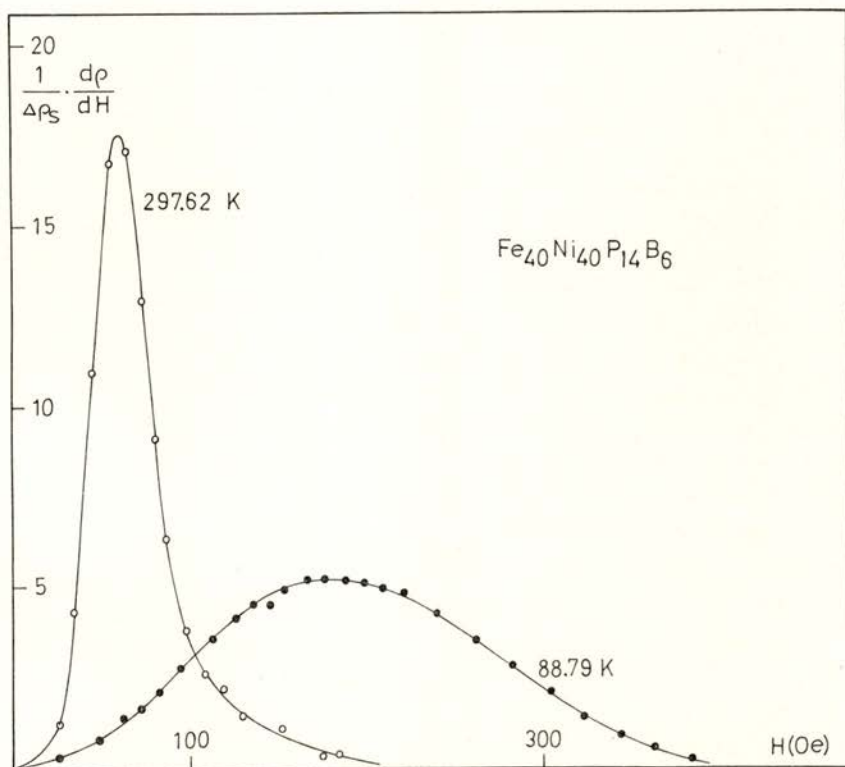


Fig. 9— Normalized field derivative  $(1 / \Delta \rho_s) \cdot (d\rho / dH)$ , as a function of the applied magnetic field ( $\mathbf{H}$ ), for a  $\text{Fe}_{40}\text{Ni}_{40}\text{P}_{14}\text{B}_6$  amorphous sample ( $\mathbf{I} \parallel \mathbf{H}$ ), at two distinct temperatures.

helimagnetic phase (\*). The final extinction of the helimagnetic structure is clearly associated with the kinks observed in our experimental curves, marking the onset of the ferromagnetic phase.

(\*) When the helimagnetic order exists, the associated magnetic periodicity (modulation vector  $\mathbf{q}$ ; period generally different from the lattice one) originates new energy gaps (less conduction electrons), thus higher electrical resistivity.

The subsequent increase of  $H$  only originates a small enhancement of the negative magneto-resistivity, due to the gradual suppression of the spin fluctuations in the system. One should notice the almost perfect parallelism between these  $\Delta \rho_{\parallel} / \rho$  curves at high fields and the one described in (i) (corresponding to an intrinsically ferromagnetic situation).

#### 4.4 — *Magneto-resistance of amorphous metals* ( $\text{Fe}_{40}\text{Ni}_{40}\text{P}_{14}\text{B}_6$ )

Although we did not consider this case in the previous sections, the magneto-resistance measurements can be very informative in the study of amorphous metals.

Fig. 9 shows the normalized field derivative  $(1/\Delta \rho_s) \cdot (d\rho/dH)$  as a function of  $H$ , at two distinct temperatures well below the Curie point;  $\Delta \rho_s$  is the saturation value of  $\Delta \rho$  in high fields [45].

The pronounced differences between the two experimental curves have been associated with important changes (with temperature) of the direction of the easy magnetization in the amorphous metallic ribbon. This assumption is compatible with the recent interpretation of Mössbauer data in  $\text{Fe}_{40}\text{Ni}_{40}\text{P}_{14}\text{B}_6$  amorphous samples [46], assuming that the easy magnetic direction changes from the ribbon plane ( $T \geq 220 \text{ K}$ ) towards a tilted configuration with respect to the ribbon plane (about  $20^\circ$ ;  $T \leq 220 \text{ K}$ ).

The authors acknowledge with pleasure financial support given by INIC (Portugal). Thanks are also due to P. P. Freitas for the contribution given in a preliminary stage of the implementation of the experimental method.

#### REFERENCES

- [1] A. H. WILSON, *The Theory of Metals*, Cambridge Univ. Press, London (1953).
- [2] J. L. OLSEN, *Electron Transport in Metals*, Interscience Publishers, N. Y. (1962).
- [3] H. M. ROSENBERG, *Low Temperature Solid State Physics*, Oxford Univ. Press (1965).
- [4] J. SMIT, *Physica*, **16**, 612 (1951).
- [5] R. M. BOZORTH, *Ferromagnetism*, D. Van Nostrand (1951).

- [6] Y. YAMADA, S. TAKADA, *J. Phys. Soc. Japan*, **34**, 51 (1973).
- [7] C. M. HURD, *Advances in Physics*, **23**, 315 (1974).
- [8] N. W. ASHCROFT, N. D. MERMIN, *Solid State Physics*, Holt, Rinehart and Winston (1976).
- [9] J. S. DUGDALE, *The Electrical Properties of Metals and Alloys*, Edward Arnold, London (1977).
- [10] J. B. SOUSA, M. M. AMADO, M. E. BRAGA, R. S. PINTO, J. M. MOREIRA, *Commun. on Physics*, **2**, 95 (1977).
- [11] T. HIRAOKA, M. SUZUKI, *J. Phys. Soc. Japan*, **31**, 1361 (1971).
- [12] D. S. SIMONS, M. S. SALOMON, *Phys. Rev.*, **B10**, 4680 (1974).
- [13] P. P. FREITAS, J. B. SOUSA, *J. Phys. F: Metal Physics*, **13**, 1245 (1983).
- [14] J. M. MOREIRA, *Ph. D. Thesis*, Univ. Porto (1985).
- [15] J. M. MOREIRA, J. B. SOUSA, J. D. MONTENEGRO, M. E. BRAGA, D. MELVILLE, *Physica*, **130 B**, 88 (1985).
- [16] L. D. LANDAU, E. M. LIFSHITZ, *Statistical Physics*, Pergamon Press, vol. V Course on Theoretical Physics (1958).
- [17] J. B. SOUSA, J. M. MOREIRA, *Portugaliae Physica*, **13**, 137 (1982).
- [18] R. I. JOSEPH, E. SCHLÖMANN, *J. Appl. Phys.*, **36**, 1579 (1965).
- [19] S. ALEXANDER, J. S. HELMAN, I. BALBERG, *Phys. Rev.*, **B13**, 304 (1976).
- [20] H. CLARK, *Solid State Physics*, MacMillan (1968).
- [21] T. G. RICHARD, D. J. W. GELDART, *Phys. Rev. Lett.*, **30**, 290 (1973).
- [22] M. E. FISHER, J. S. LANGER, *Phys. Rev. Lett.*, **20**, 665 (1968).
- [23] V. L. GINZBURG, *Sov. Physics, Solid State*, **2**, 1824 (1960).
- [24] H. E. STANLEY, *Introduction to Phase Transitions and Critical Phenomena*, Oxford Univ. Press (1971).
- [25] G. TOULOUSE, P. PFEUTY, *Introduction au Groupe de Renormalisation et à ses Applications*, Presses Univ. Grenoble (1975).
- [26] S. K. MA, *Modern Theory of Critical Phenomena*, W. A. Benjamin Inc. (1976).
- [27] N. BOCCARA, *Symétries Brisées*, Hermann (1976).
- [28] H. YAMADA, S. TAKADA, *Prog. Theor. Phys.*, **48**, 1828 (1972).
- [29] I. BALBERG, J. S. HELMAN, *Phys. Rev.*, **B18**, 303 (1978).
- [30] T. R. MCGUIRE, R. I. POTTER, *Trans. Magnetism*, **MAG-11**, 1018 (1975).
- [31] J. B. SOUSA, J. F. D. MONTENEGRO, J. M. MOREIRA, M. E. BRAGA, *J. Phys. F: Metal Physics*, **12**, 351 (1982).
- [32] E. DU TRÉMOLET DE LACHEISSERIE, *Ann. Phys.*, Paris, **5**, 267 (1970).
- [33] C. HERRING, *J. Appl. Physics*, **35**, 1939 (1960).
- [34] J. B. SOUSA, M. M. AMADO, R. P. PINTO, M. F. PINHEIRO, J. M. MOREIRA, M. E. BRAGA, M. AUSLOOS, P. CLIPPE, D. HUKIN, G. GARTON, P. WALKER, *Advances in Condensed Matter Physics*, ed J. T. Devreese, Plenum Press N. Y., vol. 4, 115 (1981).
- [35] L. BERGER, *Physica*, **30**, 1141 (1964).

- [36] J. SMIT, *Physica*, **21**, 877 (1955).
- [37] J. SMIT, *Physica*, **24**, 39 (1958).
- [38] J. SANT'OVAIA, J. B. SOUSA, Seminário, Lab. Física do Porto (1981).
- [39] A. LAGE, A. GOMES, Fac. Engenharia do Porto (1979).
- [40] J. B. SOUSA, J. M. MOREIRA, P. P. FREITAS, *Proceedings Portuguese Physics Conference 84*, Évora, page 346 (1984).
- [41] S. CHIKAZUMI, *Physics of Magnetism*, John Wiley, N. Y. (1966).
- [42] T. ITO, S. LEGVOLD, B. J. BEAUDRY, *Phys. Rev.*, **B23**, 3409 (1981).
- [43] J. B. SOUSA, J. M. MOREIRA, M. E. BRAGA, S. B. PALMER, S. BATES, B. J. BEAUDRY, *J. Phys. F.*, **16**, 1171 (1985).
- [44] D. H. MARTIN, *Magnetism in Solids*, Iliffe Books, London (1967).
- [45] J. M. MOREIRA, J. B. SOUSA, J. D. MONTENEGRO, M. E. BRAGA, *Proceedings of Portuguese Physics Conference 84*, Évora, page 312 (1984).
- [46] C. L. CHIEN, R. HASEGAWA, *J. Appl. Phys.*, **47**, 2234 (1978).